American Mineralogist, Volume 86, pages 747–751, 2001

Hardystonite from Franklin Furnace: A natural modulated melilite

LUCA BINDI,[1] MICHAEL CZANK,[2] FRANÇOIS RÖTHLISBERGER,[3,†] AND PAOLA BONAZZI[1,*]

[1] Dipartimento di Scienze della Terra, University of Florence, via La Pira 4 I-50121 Florence, Italy
[2] Institut für Geowissenschafte-Mineralogie-Olshausenstrasse 40 D-24098 Kiel, Germany
[3] Bayerisches Geoinstitut, Universität Bayreuth, D-95440 Bayreuth, Germany

ABSTRACT

Natural hardystonite, $(Ca_{1.85}Na_{0.14}Pb_{0.01})(Zn_{0.85}Al_{0.07}Mg_{0.03}Mn^{3+}_{0.04}Fe^{3+}_{0.02})Si_{2.00}O_{7.00}$, from the type locality was reinvestigated with single crystal X-ray diffraction, microprobe analysis, and electron diffraction. The average structure, space group $P\bar{4}2_1m$, $a = 7.800(1)$ Å, $c = 5.000(1)$ Å, was refined to $R = 1.91\%$ using 331 independent reflections. Hardystonite exhibits an incommensurate modulated structure. As in synthetic melilite-type compounds, modulation is two-dimensional, with tartan-like appearance; modulation vectors are $\mathbf{q_1} = \alpha(\mathbf{a_1}^* + \mathbf{a_2}^*)$ and $\mathbf{q_2} = \alpha(-\mathbf{a_1}^* + \mathbf{a_2}^*)$. A modulation wavelength $\lambda = 19.0(4)$ Å was estimated by centering satellite reflections using a single-crystal diffractometer. TEM-EDX investigations proved the chemical composition of the sample to be slightly inhomogeneous, with stronger and sharper satellites in the regions where the composition approaches the $Ca_2ZnSi_2O_7$ end-member. Geometrical parameters as well as anisotropic displacement ellipsoids of hardystonite are consistent with those of the other melilite-type compounds having a modulated character.

INTRODUCTION

The melilite group of minerals consists mainly of solid-solutions between gehlenite, $Ca_2Al_2SiO_7$, and åkermanite, $Ca_2MgSi_2O_7$. These phases are found in both plutonic and volcanic basic alkaline rocks rich in calcium, in thermally metamorphosed impure carbonate rocks, in blast-furnace slags, and in aluminum-rich chondrules of meteorites (Deer et al. 1986). Many melilite-type compounds with the general formula $X_2T1(T2)_2O_7$ (X = Ca, Sr, Pb, Ba, Na,Y, Er,Yb; T1 = Be, Mg, Mn^{2+}, Fe^{2+}, Co, Cu, Zn, Cd, Al, Fe^{3+}, Ga, Si; T2 = Si, Ge, Al, Fe^{3+}, Ga, Be) have been synthesized either from a melt, by sintering, or under hydrothermal conditions (Röthlisberger et al. 1990). Several crystal structure refinements on synthetic compounds with a wide range of chemical compositions have been published (Bartram 1969; Louisnathan 1970; Kimata and Ii 1981, 1982; Kimata and Ohashi 1982; Kimata 1983a, 1983b, 1984, 1985; Armbruster et al. 1990; Shimizu et al. 1995; Yang et al. 1997). However, comparatively, few natural melilites have been studied (Warren 1930; Smith 1953; Louisnathan 1971; Cruciani and Vaccaro 1996; Giuli et al. 2000).

Hemingway et al. (1986) observed satellite reflections and thermal behavior anomalies in synthetic $Ca_2MgSi_2O_7$. Seifert et al. (1987) reported electron diffraction patterns and TEM images of synthetic iron-bearing åkermanites exhibiting two-dimensional incommensurately modulated structure. They also suggested that the formation of the incommensurate phase is due to a structural misfit between tetrahedral sheet and the X-polyhedral layer. Röthlisberger et al. (1990) pointed out the role of the chemical composition in the stabilization of the incommensurate phase. By means of an electron diffraction and electron microscopy study of synthetic $Ca_2ZnGe_2O_7$, Van Heurck et al. (1992) showed the structure to be modulated by the formation of microdomains involving different orientations of the T1 and T2 tetrahedra. According to Seifert and Röthlisberger (1993) the modulation amplitude is temperature-dependent and the dynamic disorder of the X cations may lead to the stabilization of the unmodulated melilite structure at high temperatures only. From the theoretical principles of the incommensurability in crystals (Janssen and Janner 1987), the incommensurate phases are intermediate between a commensurate high-temperature phase (unmodulated structure) and a low-temperature commensurate superstructure (the so called "lock-in phase"). Riester and Böhm (1997) found the "lock-in phase" of Co-åkermanite to occur at 130 K. The result is a nearly commensurate phase ($3a \times 3a \times c$ supercell), with clusters of 6- and 7-fold coordinated calcium arranged in octagons (Riester et al. 2000). On the basis of a five-dimensional refinement of the modulated phase, Hagiya et al. (1993) and Kusaka et al. (1998) concluded that modulation in synthetic compounds [Co-åkermanite and $Ca_2(Mg_{0.55}Fe_{0.45})Si_2O_7$] results from static displacement of the constituent atoms from their dynamically-averaged positions, that is, modulation arises from positional and not substitutional disorder. In contrast, Jiang et al. (1998) postulated that occupational modulation makes a contribution to the overall modulation characteristics, as a consequence of an ordered distribution of Sr in $(Ca_{1-x}Sr_x)_2MgSi_2O_7$. Occupancy modulation of Sr and Ca was observed also by Bagautdinov et al. (2000) who refined the incommesurately modulated structure of $(Sr_{0.13}Ca_{0.87})_2CoSi_2O_7$. A formal solution to the problem of the modulated structure in melilites was provided by

* E-mail: pbcry@steno.geo.unifi.it
† Present address: Champ Martin 2, CH-2735 Malleray, Switzerland.

McConnell (1999), indicating the coexistence of two structurally distinct components ($P\bar{4}$ and $P2_12_12$) in the incommensurate phase.

According to the systematic relationship between chemical composition and the IC-normal phase transition temperature, melilites close to the hardystonite $Ca_2ZnSi_2O_7$ end-member should exhibit a modulated structure at room temperature. Previous X-ray studies on such natural melilites (Warren and Trautz 1930, Louisnathan 1969) however, did not detect such a phenomenon. We therefore re-examined natural hardystonite also from the type locality (Franklin Furnace, New Jersey, USA), by single-crystal X-ray diffraction, microprobe analysis and electron diffraction.

Experimental methods

A crystal of hardystonite was selected and mounted on an Enraf-Nonius CAD4 diffractometer. 25 high-θ reflections were centered and subsequently indexed yielding a = 7.800(1) Å, c = 5.000(1) Å, V = 304.20 (2) Å^3. Taking what was previously observed in melilite-type modulated structures into account (Van Heurck et al. 1992), we looked for satellite reflections on the basis of a 7 × 7 square grid subdividing the reciprocal basic cell. The presence of satellites at approximately 2/7 and 5/7 along $[110]_{basic}$ and $[1\bar{1}0]_{basic}$ was confirmed; weaker satellites along $[100]_{basic}$ and $[010]_{basic}$ at approximately 3/7 and 4/7 were also observed. Other hardystonite crystals tested gave quite similar results. As in synthetic melilite-type compounds, modulation is two-dimensional, with tartan-like appearance; modulation vectors are $\mathbf{q_1} = \alpha(\mathbf{a_1}^* + \mathbf{a_2}^*)$ and $\mathbf{q_2} = \alpha(-\mathbf{a_1}^* + \mathbf{a_2}^*)$; to estimate α, four pairs of centrosymmetric satellite reflections were centered and an average value α = 0.291(6) was obtained, corresponding to a modulation wavelength λ = 19.0(4) Å. Intensity of both main and satellite reflections were measured using a Enraf-Nonius CAD4 diffractometer. Data were subsequently corrected for Lorentz-polarization and for absorption according to the semiempirical method of North et al. (1968). Experimental details are given in Table 1. In Figure 1 the IC-satellites in two layers of the reciprocal space (l = 0, l = 1) are schematically represented. The tetragonal symmetry appears to be violated by some of the satellites, probably due to the low quality counting statistics for weak peaks.

Table 1. Experimental details of data collection

	a	b
wavelength	Mo$K\alpha$ (20 mA × 50 kV)	Mo$K\alpha$ (26 mA × 50 kV)
scan mode	ω	ω/2θ
scan width (°)	3.5	1.8
scan speed (°/min)	4.12	2.75
θ-range (°)	2–30	2–18

Notes: a = basic structure reflections; b = IC modulated structure reflections

For the TEM investigations, a small piece of the sample was ground in an agate mortar, suspended in ethanol and dispersed in an ultrasonic bath. The fine fraction was then deposited onto a holey carbon film. The TEM used was a Philips EM400T microscope (Kiel University) operated at 100 kV and equipped with a rotation-tilt (360°, ± 60°) sample holder. An attached energy dispersive spectrometer allowed qualitative chemical analyses and a check for homogeneity.

Structure refinement

The basic structure of hardystonite was refined by means of the program SHELXL 93 (Sheldrick 1993). Equivalent reflections were merged (R_{symm} = 6.43%) according to the symmetry of the basic structure ($P\bar{4}2_1m$ space group). By means of some anisotropic full-matrix least-squares cycles, the refinement quickly converged to R = 1.91 % for 331 observed reflections [all the reflections resulted "observed" according to the criterion $Fo > 4\sigma(Fo)$]. The scattering curves for neutral Ca,

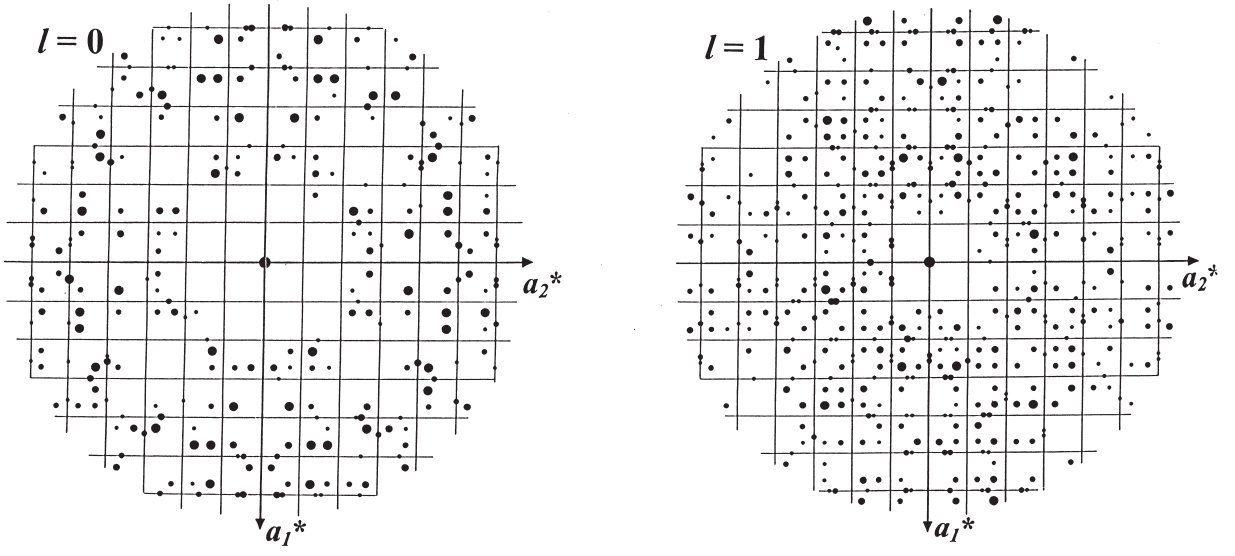

Figure 1. Schematic representation of IC-satellites in two layers of the reciprocal space (l = 0, l =1). The size of the dots is roughly proportional to Fo/σ(Fo), [Fo/σ(Fo) > 40, 20, 10, and 5, respectively]. Basic reflections are omitted. Grid refers to basic lattice.

Na, Zn, Mg, Si, O were taken from *International Tables for X-ray Crystallography*, volume IV (Ibers and Hamilton 1974). The site-occupancy refinement for the T1 and X sites led to a mean electron number of 28.2, and 19.9 respectively. Atomic coordinates and anisotropic displacement parameters are given in Table 2.

CHEMICAL COMPOSITION

The same crystal used for the structure refinement was analysed by means of a Jeol JXA-8600 electron microprobe. Major and minor elements were determined at 15 kV accelerating voltage and 10 nA beam current, with variable counting times: 15 s were used for Na, 20 s for other major elements and 30 s for the minor elements Al, Mn, Fe, Mg, and Pb. The standards were: willemite (Zn), olivine (Mg), diopside (Ca), albite (Al, Si, Na), bustamite (Mn), ilmenite (Fe), sanidine (K), and galena (Pb). The average chemical composition (nine analyses on different spots) is reported in Table 3. On the basis of five cations, the formula of the hardystonite is $(Ca_{1.85}Na_{0.14}Pb_{0.01})(Zn_{0.85}Al_{0.07}Mg_{0.03}Mn_{0.04}Fe_{0.02})Si_{2.00}O_{7.00}$. To achieve electric neutrality, Mn and Fe were assumed to be trivalent. The mean electron numbers calculated for the site population obtained on the basis of the chemical data (19.6 for the X site and 28.0 for the T1 site) are in close agreement with those from the site occupancy refinement (19.9 and 28.2 respectively).

TEM INVESTIGATIONS

In electron diffraction, the satellite peaks typical for the modulated phase could be observed (e.g., Seifert et al. 1987). The sample proved, however, to be slightly inhomogeneous and distinctly bimodal on the scale of a few hundred nanometers (i.e., below the spatial resolution of the microprobe), both with respect to modulation and chemistry: Grains with only very minor concentrations of elements except Ca, Zn, Si and O exhibited strong and sharp satellite peaks with locations corresponding to a modulation wavelength on the [110] direction of 19.6(1) Å (Fig. 2a). Other grains showed weaker and diffuse

TABLE 3. Electron microprobe analyses (means, ranges and standard deviations in wt% of oxides) and atomic ratios (on the basis of five cations) for hardystonite

oxide	wt%	range	σ%	atom	atomic ratios
SiO_2	38.93	38.77–39.27	0.11	Si	2.004
Al_2O_3	1.14	0.97–1.22	0.04	Al	0.069
Mn_2O_3	1.00	0.76–1.12	0.06	Mn	0.039
Fe_2O_3	0.43	0.18–0.52	0.05	Fe	0.017
MgO	0.36	0.18–0.43	0.04	Mg	0.028
ZnO	22.44	22.09–23.05	0.25	Zn	0.853
CaO	33.47	33.12–34.40	0.01	Ca	1.846
PbO	0.58	0.37–0.70	0.04	Pb	0.008
Na_2O	1.36	0.85–1.52	0.05	Na	0.136
total	99.71			Σ_{ch}	13.997

Note: Σ_{ch} = sum of cation charge, assuming Fe and Mn as trivalent.

TABLE 2. Fractional atomic coordinates and anisotropic displacement parameters U_{ij} (Å^2) for hardystonite

	x/*a*	*y*/*b*	*z*/*c*	U_{11}	U_{22}	U_{33}	U_{12}	U_{13}	U_{23}	U_{eq}
X	0.3326(1)	$^1/_2$ – x	0.5059(1)	0.0240(3)	U_{11}	0.0140(2)	0.0104(3)	0.0016(2)	$-U_{13}$	0.0206(2)
T1	0	0	0	0.0125(2)	U_{11}	0.0127(3)	0	0	0	0.0126(2)
T2	0.1400(1)	$^1/_2$ – x	0.9386(1)	0.0124(3)	U_{11}	0.0099(4)	0.0006(4)	0.0005(2)	$-U_{13}$	0.0116(2)
O1	0.5000	0	0.1777(7)	0.038 (2)	U_{11}	0.009 (1)	–0.026 (2)	0	0	0.0284(9)
O2	0.1410(3)	$^1/_2$ – x	0.2569(4)	0.027 (1)	U_{11}	0.011 (1)	0.010 (1)	–0.002 (1)	$-U_{13}$	0.0217(6)
O3	0.0820(3)	0.1872(3)	0.7867(4)	0.045 (1)	0.020 (1)	0.017 (1)	–0.010 (1)	0.009 (1)	–0.003 (1)	0.0273(5)

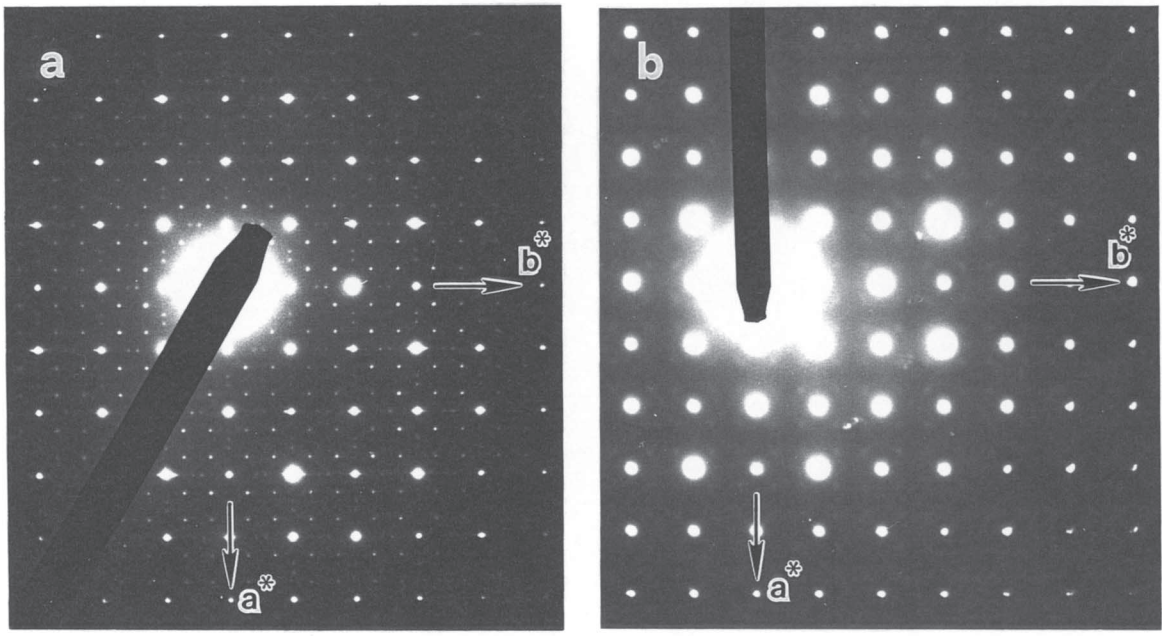

FIGURE 2. SAED patterns of hardystonite from Franklin Furnace. Stronger and sharper satellites are observed in the regions where composition approaches the $Ca_2ZnSi_2O_7$ end-member (**a**); Pb-richer regions (**b**) exhibit weaker and diffuse satellites. Electron beam along [001].

satellites, indicating a wavelength close to 20.6(2) Å, and significant (but still fairly low) concentrations of Pb, Mn and Ni (Fig. 2b).

DISCUSSION

On the whole, the previously determined structure of hardystonite was confirmed. It consists of a two-dimensional linkage of corner sharing T1 and T2 tetrahedra, characterized by irregular pentagonal rings. In the stacking of successive tetrahedral layers along [001], the pentagonal rings form channels where the X cations are located about halfway between the sheets. The *c* parameter corresponds to one layer of interconnected tetrahedra. Selected bond distances and angles are in Table 4. The X site in hardystonite from Franklin Furnace deposit is dominated by Ca with minor amounts of Na and Pb. Accordingly, the mean <X-O> distance (2.562 Å) is nearly equal to that observed by Louisnathan (1969) for hardystonite from Franklin Furnace slags (2.569 Å). The T1 site is mainly occupied by Zn, with minor amounts of Al, Mg, Mn, and Fe. The mean <T1-O> distance (1.918 Å) is significantly shorter than that (1.937 Å) found by Louisnathan (1969), probably due to the greater amount of Al in the present sample. The mean <T2-O> bond distance (1.617 Å) is within the range (1.608 – 1.623 Å) observed for <Si-O> distances in the compounds where T2 is completely filled by Si, e.g. in synthetic åkermanite (Kimata and Ii 1981), Co-åkermanite (Kimata 1983b) and gugiaite (Kimata and Ohashi 1982). This feature, as well as the chemical data (atomic ratios close to 2.00 a.p.f.u of Si), suggests that the T2 site is completely filled by Si.

As pointed out by Seifert et al. (1987), geometrical restrictions exist in terms of the size of the tetrahedral cations with respect to the size of the interlayer X cations (Ca, Sr, Ba, Y, etc.). The greater the hindrance of tetrahedra relative to X-polyhedra, the bigger the structural strain and the consequent deformation of the tetrahedral sheet. Therefore, the T/X ratio, with T/X = [(<T1-O> + 2<T2-O>) / 3<X-O>], can be an useful parameter to predict the possible presence of an incommensurate modulation in melilite-type structures. In particular, both the value of the T1-O3-T2 angle and the angular distortion σ^2_{T2}, plotted against the T/X ratio (Giuli et al. 2000), are helpful to discriminate the melilite-type structures with incommensurate modulation from the others. As shown in Figure 3, the crystal chemical behavior of the hardystonite studied here is consistent with that of other melilites having modulated character. The TEM observation of diffuse satellites in Pb-rich grains versus sharp peaks in Pb-poor grains is consistent with the above concept that an increase in the average size of the X cation destabilizes the incommensurately modulated structure (Röthlisberger et al. 1990).

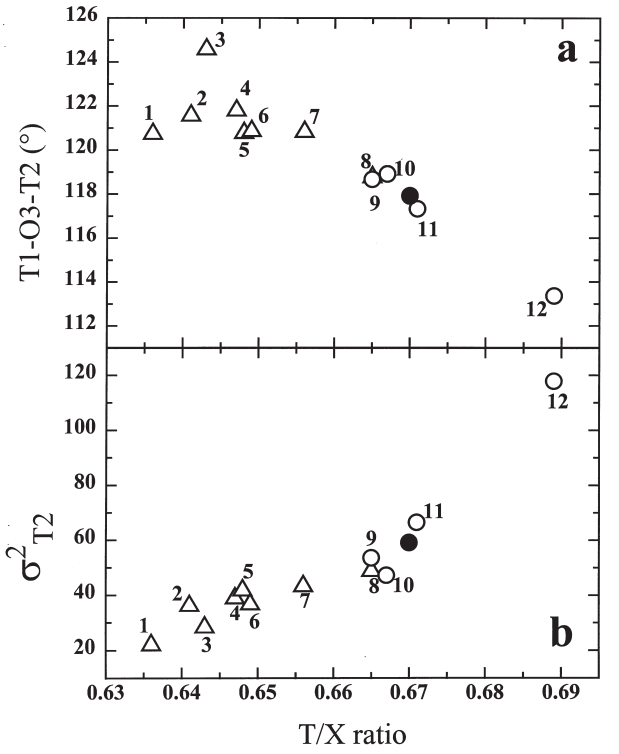

FIGURE 3. Values of T1-O3-T2 angle (**a**) and angular distortion σ^2 for T2 tetrahedron (**b**) plotted against the T/X ratio (see text). Filled circle refers to this study. Open symbols refer to the literature: (1) $Ca_2SiB_2O_7$ Giuli et al. 2000; (2) $Sr_2Al_2SiO_7$ Kimata 1984; (3) $Ba_2MgSi_2O_7$ Shimizu et al. 1995; (4) $Sr_2MgSi_2O_7$ Kimata 1983a; (5) $Ca_2BeSi_2O_7$ Kimata and Ohashi 1982; (6) $CaNaAlSi_2O_7$ Louisnathan 1970; (7) $Sr_2MnSi_2O_7$ Kimata 1985; (8) $Ca_2Al_2SiO_7$ Kimata and Ii 1982; (9) $Ca_2CoSi_2O_7$ Kimata 1983b; (10) $Ca_2MgSi_2O_7$ Kimata and Ii 1981; (11) $Ca_2ZnSi_2O_7$ Louisnathan 1969; (12) $Ca_2ZnGe_2O_7$ Armbruster et al. 1990. Structures with proved modulated character are indicate with empty circles.

TABLE 4. Selected bond distances (Å) and interatomic angles (°) in hardystonite

X-O1	2.470(3)	O3-T1-O3' [×4]	108.01(4)
X-O2	2.453(3)	O3-T1-O3" [×2]	112.43(5)
X-O2' [×2]	2.690(2)		
X-O3 [×2]	2.412(2)	O1-T2-O2	111.03(4)
X-O3' [×2]	2.685(3)	O1-T2-O3 [×2]	101.63(5)
		O2-T2-O3 [×2]	117.93(4)
T1-O3 [×4]	1.918(2)	O3-T2-O3'	104.32(4)
σ^2_{T1}	5.21		
		T2-O1-T2'	138.73(4)
T2-O1	1.650(2)	T1-O3-T2	117.92(5)
T2-O2	1.592(3)		
T2-O3 [×2]	1.612(2)		
σ^2_{T2}	59.13		
λ_{T2}	1.0133		

Note: The mean quadratic elongation (λ) and the angle variance (σ^2) were computed according to Robinson et al. (1971).

The incommensurate modulation is also evident in the analysis of the size and the shape of the displacement ellipsoids. As Armbruster et al. (1990) pointed out, the strong anisotropy for the displacement ellipsoids of O1 and O3 O atoms in the average structure of melilites is related to the incommensurate modulation. This feature indicates wide disorder in the orientation of the tetrahedra on the scale of the tetragonal unit cell. Therefore, d_{maxO1} and d_{maxO3} were calculated according to the formulae proposed by Armbruster et al. (1990). These values, 0.15 for O1 and 0.12 for O3, are close to those observed by Armbruster et al. (1990) for melilites showing IC satellites (0.11–0.32 and 0.12–0.39 for d_{maxO1} and d_{maxO3}, respectively).

ACKNOWLEDGMENTS

The authors are grateful to F. Seifert for critical reading of the manuscript. Thanks are also due to F.Olmi (CNR - Centro di Studio per la Minerogenesi e la Geochimica Applicata-Firenze) for his help in electron microprobe analyses. This work was funded by M.U.R.S.T., cofinanziamento 1999, project "Transformations, reactions, ordering in minerals" and German Science Foundation (DFG).

REFERENCES CITED

Armbruster, T., Röthlisberger, F., and Seifert, F. (1990) Layer topology, stacking variation, and site distortion in melilite-related compounds in the system CaO-ZnO-GeO_2-SiO_2. American Mineralogist, 75, 847–858.

Bagautdinov, B., Hagiya, K., Kusaka, K., Ohmasa, M., and Iishi, K. (2000) Two-dimensional incommensurately modulated structure of $(Sr_{0.13}Ca_{0.87})_2CoSi_2O_7$ crystals. Acta Crystallographica, B56, 811–821.

Bartram, S.F. (1969) Crystal structure of $Y_2SiBe_2O_7$. Acta Crystallographica, B25, 791–795.

Cruciani, G. and Vaccaro, C. (1996) La melilite nei filoni basici di Tapira (Brasile): analisi strutturale e significato petrologico (abstract). Plinius, 16, 85–86.

Deer, W.A., Howie, R.A., and Zussman, J. (1986) Rock-forming minerals. Vol. 1b: Disilicates and ring silicates. 2nd Ed. Longman, Harlow, G.B.

Giuli, G., Bindi, L., and Bonazzi, P. (2000) Rietveld refinement of okayamalite, $Ca_2SiB_2O_7$: Structural evidence of B/Si distribution. American Mineralogist, 85, 1512–1515.

Hagiya, K., Ohmasa, M., and Iishi, K. (1993) The modulated structure of synthetic Co-åkermanite, $Ca_2CoSi_2O_7$. Acta Crystallographica, B49, 172–179.

Hemingway, B.S., Evans, H.T.Jr., Nord, G.L.Jr., Haselton, H.T.Jr., Robie, R.A., and McGee, J.J. (1986) Åkermanite: phase transitions in heat capacity and thermal expansion, and revised thermodynamic data. Canadian Mineralogist, 24, 425–434.

Ibers, J.A. and Hamilton, W.C. Eds. (1974) International Tables for X-ray Crystallography, vol. IV, 366 p. Kynock, Dordrecht, the Netherlands.

Janssen, Y. and Janner, A. (1987) Incommensurability in crystals. Advances in Physics, 36, 519–624.

Jiang, J.C., Schosnig, M., Schaper, A.K., Ganster, K., Rager, H., and Tóth, L. (1998) Modulations in incommensurate $(Ca_{1-x}Sr_x)_2MgSi_2O_7$ single crystals. Physics and Chemistry of Minerals, 26, 128–134.

Kimata, M. (1983a) The structural properties of synthetic Sr-åkermanite, $Sr_2MgSi_2O_7$. Zeitschrift für Kristallographie, 163, 295–304.

———(1983b) The crystal structure and stability of Co-åkermanite, $Ca_2CoSi_2O_7$, compared with the mineralogical behaviour of Mg cation. Neues Jahrbuch für Mineralogie Abhandlungen, 146, 221–241.

———(1984) The structural properties of synthetic Sr-gehlenite, $Sr_2Al_2SiO_7$. Zeitschrift für Kristallographie, 167, 103–116.

———(1985) The structural properties and mineralogical significance of synthetic $Sr_2MnSi_2O_7$ melilite with 4-coordinated manganese. Neues Jahrbuch für Mineralogie Monatshefte, 1985, 85–96.

Kimata, M. and Ii, N. (1981) The crystal structure of synthetic åkermanite, $Ca_2MgSi_2O_7$. Neues Jahrbuch für Mineralogie Monatshefte, 1981, 1–10.

———(1982) The structural property of synthetic gehlenite, $Ca_2Al_2SiO_7$. Neues Jahrbuch für Mineralogie Abhandlungen, 144, 254–267.

Kimata, M. and Ohashi, H. (1982) The crystal structure of synthetic gugiaite, $Ca_2BeSi_2O_7$. Neues Jahrbuch für Mineralogie Abhandlungen, 143, 210–222.

Kusaka, K., Ohmasa, M., Hagiya, K., Iishi, K., and Haga, N. (1998) On variety of the Ca coordination in the incommensurate structure of synthetic iron-bearing åkermanite, $Ca_2(Mg_{0.55},Fe_{0.45})Si_2O_7$. Mineralogical Journal, 20, nr. 2, 47–58.

Louisnathan, S.J. (1969) Refinement of the crystal structure of hardystonite, $Ca_2ZnSi_2O_7$. Zeitschrift für Kristallographie, 130, 427–437.

———(1970) The crystal structure of synthetic soda melilite, $CaNaAlSi_2O_7$. Zeitschrift für Kristallographie, 131, 314–321.

———(1971) Refinement of the crystal structure of a natural gehlenite, $Ca_2Al(Al,Si)_2O_7$. Canadian Mineralogist, 10, 822–837.

McConnell, J.D.C. (1999) The analysis of incommensurate structures in terms of full space group theory, and the application of the method to melilite. Zeitschrif für Kristallographie, 214, 457–464.

North, A.C.T., Phillips, D.C., and Mathews, F.S. (1968) A semiempirical method of absorption correction. Acta Crystallographica, A24, 351–359.

Riester, M. and Böhm, H. (1997) Phase transitions of modulated Co-åkermanite, $Ca_2CoSi_2O_7$. Zeitschrift für Kristallographie, 212, 506–509.

Riester, M., Böhm, H., and Petricek, V. (2000) The commensurately modulated structure of the lock-in phase of synthetic Co-åkermanite, $Ca_2CoSi_2O_7$. Zeitschrift für Kristallographie, 215, 102–109.

Robinson, K., Gibbs, G.V., and Ribbe, P.H. (1971) Quadratic elongation; a quantitative measure of distortion in coordination polyhedra. Science, 172, 567–570.

Röthlisberger, F., Seifert, F., and Czank, M. (1990) Chemical control of the commensurate-incommensurate phase transition in synthetic melilites. European Journal of Mineralogy, 2, 585–594.

Seifert, F. and Röthlisberger, F. (1993) Macroscopic and structural changes at the incommensurate-normal phase transition in melilites. Mineralogy and Petrology, 48, 179–192.

Seifert, F., Czank, M., Simons, B., and Schmahl, W. (1987) A commensurate-incommensurate phase transition in iron-bearing åkermanite. Physics and Chemistry of Minerals, 14, 26–35.

Sheldrick, G.M. (1993) SHELXL-93: A new structure refinement program. University of Gottingen, Germany.

Shimizu, M., Kimata, M., and Iida, I. (1995) Crystal structure of $Ba_2MgSi_2O_7$: the longest tetrahedral Mg-O distance. Neues Jahrbuch für Mineralogie Monatshefte, 1995, 39–47.

Smith, J.V. (1953) Reexamination of the crystal structure of melilite. American Mineralogist, 38, 643–661.

Van Heurck, C., Van Tendeloo, G., and Amelinckx, S. (1992) The modulated structure in the melilite $Ca_2ZnGe_2O_7$. Physics and Chemistry of Minerals, 18, 441–452.

Warren, B.E. (1930) The structure of melilite $(Ca,Na)_2(Mg,Al)_1(Si,Al)_2O_7$. Zeitschrift für Kristallographie, 74, 131–138.

Warren, B.E. and Trautz, O.R. (1930) The structure of hardystonite $Ca_2ZnSi_2O_7$. Zeitschrift für Kristallographie, 75, 525–528.

Yang, H., Hazen, R.M., Downs, R.T., and Finger, L.W. (1997) Structural change associated with the incommensurate-normal phase transition in åkermanite, $Ca_2MgSi_2O_7$, at high pressure. Physics and Chemistry of Minerals, 24, 510–519.

MANUSCRIPT RECEIVED FEBRUARY 7, 2000
MANUSCRIPT ACCEPTED JANUARY 26, 2001
MANUSCRIPT HANDLED BY ANNE M. HOFMEISTER